

The Solution Structure of FADD Death Domain

STRUCTURAL BASIS OF DEATH DOMAIN INTERACTIONS OF Fas AND FADD*

(Received for publication, February 8, 1999, and in revised form, March 27, 1999)

Eui-Jun Jeong^{‡§¶}, SookHee Bang^{‡¶||}, Tae Ho Lee^{**}, Young In Park[§], Woong-Seop Sim^{||}, and Key-Sun Kim^{‡ ‡‡}

From the [‡]Structural Biology Center, Korea Institute of Science and Technology, Seoul, 130-650, [§]the Graduate School of Biotechnology and ^{||}Department of Biology, Korea University, Seoul, 136-701, and ^{**}Department of Biology, Yonsei University, Seoul, 120-749, Korea

A signal of Fas-mediated apoptosis is transferred through an adaptor protein Fas-associated death domain protein (FADD) by interactions between the death domains of Fas and FADD. To understand the signal transduction mechanism of Fas-mediated apoptosis, we solved the solution structure of a murine FADD death domain. It consists of six helices arranged in a similar fold to the other death domains. The interactions between the death domains of Fas and FADD analyzed by site-directed mutagenesis indicate that charged residues in helices $\alpha 2$ and $\alpha 3$ are involved in death domain interactions, and the interacting helices appear to interact in anti-parallel pattern, $\alpha 2$ of FADD with $\alpha 3$ of Fas and *vice versa*.

Activation of Fas receptor (called also CD95 or APO-1) with either Fas ligand or anti-Fas antibody induces receptor clustering. This recruits the adaptor molecule FADD¹/MORT1 and procaspase-8 to the Fas receptor through the homotypic interactions of death domains (DDs) and death effector domains (DEDs), respectively, leading to proteolytic activation of caspase-8 (1–5). The activation of caspase-8 initiates a cascade of caspases and leads to cell death. The clustering of Fas receptor, FADD, and procaspase-8, termed death-inducing signaling complex, is essential for Fas-mediated apoptosis and caspase-8 activation (6) (7). In the death-inducing signaling complex formation, FADD mediates signals from Fas receptor to procaspase-8 with its C-terminal DD and N-terminal DED. FADD also participates in signaling other members of the TNFR family. FADD binds to TNFR1-associated death domain protein (TRADD), which interacts with the stimulated TNFR1 in TNF-mediated apoptosis (8). Several viral and cellular procaspase-8-like proteins, FLIPs (FLICE inhibitory proteins),

also bind to FADD and modulate Fas-induced apoptosis (9–14). Among the Fas-binding proteins, FADD is the only protein found in the death-inducing signaling complex (6) and has shown to be essential *in vivo* by use of FADD-deficient cells that are completely resistant to Fas-mediated apoptosis (15, 16). FADD is also implicated in embryo development (15), T-cell proliferation (16), and TNF-induced activation of acid sphingomyelinase (17). The downstream signal transduction of Fas- or TNF-mediated apoptosis is blocked by the N-terminal-truncated FADD that lacks death effector domain (18).

FADD exists in the cytoplasm of normal cells, but it does not induce cell death except at a high concentration (1). This suggests that the signal transduction of FADD be triggered by interactions of death domains of Fas and FADD, possibly converting FADD into a form capable of recruiting procaspase-8. However, the mechanism of a signal transduction by FADD is not yet clear. To understand the mechanism of FADD-mediated signal transduction, we determined the solution structure of a murine FADD (2) death domain (FADD-DD), carried out site-directed mutageneses, and analyzed the effect of mutagenesis on the binding affinity of FADD-DD for Fas-DD to map an interaction site of death domains. Thus far, the structures of Fas-DD (19), FADD-DED (20), and caspase recruitment domain of RAIDD (21) has been determined and known to have similar global folds. It has been suggested that the interactions between DDs or caspase recruitment domains are electrostatic (19) (21), whereas those between DEDs are hydrophobic (20). But the mode of interactions has not been clear because the information about the counter-interacting domain has not been available. By determining structure of FADD-DD, we now are able to propose a model for the death domain interactions of Fas and FADD based on the structures of Fas-DD (19), FADD-DD, and mutagenesis experiments.

MATERIALS AND METHODS

Sample Preparation—Recombinant FADD was prepared from the murine FADD gene subcloned into an expression vector pET3d (Novagen) in *Escherichia coli* strain BL21 (DE3). When cell growth is reached at the logarithmic phase at 37 °C, protein expression was induced by adding 0.4 mM isopropyl-1-thio- β -D-galactopyranoside for 3 h. The harvested cell paste was disrupted by a sonicator in a lysis buffer (50 mM Tris-HCl, pH 8.0, 1 mM EDTA, 1 mM dithiothreitol, 10% glycerol, and 1 mM phenylmethylsulfonyl fluoride), and ammonium sulfate up to 30% was added to the soluble fraction of the cell extract. The precipitant was collected by centrifugation and dialyzed overnight at pH 4.0 and further purified by reverse phase high performance liquid chromatography using a C₈ Vydac column. Purified FADD was subjected to proteolytic digestion for 2 h at 15 °C by adding subtilisin of one-hundredth of FADD in phosphate buffer at pH 8.0. The molecular weight and N-terminal amino acid sequence of the resistant fragments were analyzed, and the corresponding DNA fragments were subcloned into a pET15b expression vector. The C-terminal fragment of FADD protein (FADD-DD) was expressed in *E. coli* strain BL21 (DE3) by inducing with 0.4 mM isopropyl-1-thio- β -D-galactopyranoside for 3 h at 28 °C. The protein

* This work is supported by Biotech-2000 and KIST-2000 program (to K.-S. K.) from the Ministry of Science and Technology (MOST) of Korea. The costs of publication of this article were defrayed in part by the payment of page charges. This article must therefore be hereby marked "advertisement" in accordance with 18 U.S.C. Section 1734 solely to indicate this fact.

The atomic coordinates and structure factors (codes Ifad and rlfadmr) have been deposited in the Protein Data Bank, Brookhaven National Laboratory, Upton, NY.

¶ These authors contributed equally to this work.

‡‡ To whom correspondence should be addressed. Tel.: 82-2-958-5934; Fax: 82-2-958-5939; E-mail: keysun@kist.re.kr.

¹ The abbreviations used are: FADD, Fas-associated death domain protein; DD, death domain; DED, death effector domain; TNFR, tumor necrosis factor receptor; TRADD, TNFR1-associated death domain protein; RAIDD, RIP-associated ICH-1/CED-3-homologous protein with a death domain; NOE, nuclear Overhauser effect; NOESY, NOE enhancement spectroscopy; HSQC, heteronuclear single-quantum coherence; TOCSY, total correlation spectroscopy.

was purified by an affinity chromatography with nickel nitrilotriacetic acid-agarose column (Qiagen). The polyhistidine tag was removed by thrombin and further purified by gel filtration in ammonium acetate buffer at pH 4.0. Purified protein that has an N-terminal cloning artifact of Gly-Ser-His-Met was lyophilized and stored at -20°C . A uniformly ^{15}N and/or ^{13}C -labeled protein was prepared from cells grown in M9 minimal medium containing 1 g of $^{15}\text{NH}_4\text{Cl}$ /liter and/or 2.0 g of $[\text{U-}^{13}\text{C}]\text{glucose}$ /liter. NMR samples were prepared by dissolving about 10 mg of protein in 0.5 ml of 50 mM sodium acetate buffer composed of either 90% H_2O , 10% $^2\text{H}_2\text{O}$, or 99.9% $^2\text{H}_2\text{O}$, and the pH was adjusted to 4.00 ± 0.05 (glass electrode, uncorrected) with concentrated NaOH .

NMR Spectroscopy—The heteronuclear NMR experiments were carried out with a ^{15}N and/or ^{13}C -labeled sample in 90% H_2O , 10% $^2\text{H}_2\text{O}$ using Varian UNITYplus 600 (in Advanced Analysis Center in KIST) or Inova 500 (University of Alberta) spectrometers at 30°C . The protein concentration was about 2 mM. Once FADD-DD protein is dissolved in water for more than a week, NMR signal begins to lose its intensity, indicating the tendency of aggregation. So all experiments were carried out within a week after dissolution. Deuterium exchange of amide protons in FADD-DD was initiated by dissolving lyophilized sample in $^2\text{H}_2\text{O}$, and two-dimensional ^1H - ^{15}N HSQC spectra were recorded at 20°C , pH 4.0. After 1 h at 20°C , the temperature was increased to 30°C , and spectra were acquired. According to cross-peaks intensity remaining in each spectrum, exchange rates were divided into four groups. Two-dimensional ^1H - ^{13}C constant time-HSQC, three-dimensional ^1H - ^{15}N NOESY-HSQC, ^1H - ^{15}N TOCSY-HSQC (22), HNHA (23) were acquired with the ^{13}C - or ^{15}N -labeled sample, and ^{13}C -, ^{15}N -edited NOESY (24), CBCA(CO)NH, HNCACB (25), and ^1H - ^{15}N HCCH-TOCSY (26) were acquired with the ^{13}C -, ^{15}N -labeled sample. NMR data were processed using a program NMRPipe (27).

Assignments and Distance Restraints—Starting with identifications of ^{15}N and HN chemical shifts in ^1H - ^{15}N HSQC, spin systems were partly identified in ^1H - ^{15}N TOCSY-HSQC, and the sequential assignments of each amino acid were made using ^1H - ^{15}N NOESY-HSQC. The ^{13}C chemical shifts of each amino acid were assigned in ^1H - ^{13}C CT-HSQC and HCCH-TOCSY and verified by HNCACB and CBCA(CO)NH. Stereospecific assignments of $\text{H}\beta$ protons, and methyl groups of Val and Leu were based on the intensity of HN- $\text{H}\beta$ or HN-H γ cross-peaks in ^1H - ^{15}N TOCSY-HSQC and ^1H - ^{15}N NOESY-HSQC spectra (28) and NOE intensity of the stereospecifically assigned $\text{H}\beta$ protons to δ -methyl protons of Leu. NOE distance restraints were derived from three-dimensional ^1H - ^{15}N NOESY-HSQC, ^{13}C -, ^{15}N -edited NOESY, and ^1H NOESY spectra in $^2\text{H}_2\text{O}$, all with a mixing time of 75 or 150 ms. Only cross-peaks observed in 75 ms mixing time were used for the initial structure calculation to exclude a spin diffusion artifact. All NOE cross-peaks were assigned using a program PIPP. The NOE intensity was converted into three groups of classes (1.8–2.7, 1.8–3.5, 1.8–5.0), and pseudo-atom corrections were made appropriately (29).

Other Restraints—The scalar coupling constant of the α -proton to the amide proton was obtained from the HNHA experiments. The backbone torsion angle ϕ was restrained to -85 to -25 for $^3\text{J}_{\text{HNH}\alpha} < 5.5$ Hz, -60 to -180 for $^3\text{J}_{\text{HNH}\alpha}$ 7–8 Hz, -70 to -170 for $^3\text{J}_{\text{HNH}\alpha}$ 8–9 Hz, and -90 to -150 for $^3\text{J}_{\text{HNH}\alpha} > 9$ Hz. The ψ torsion angles of helix region were restrained to -70 to -10 . The side chain torsion angles χ_1 were restrained based on cross-peak intensities deduced from ^1H - ^{15}N HSQC-TOCSY and ^{13}C -, ^{15}N -edited NOESY spectra. Additional backbone H-bond restraints were given where secondary structures were indicated based on NOE connectivity. For each hydrogen bond, two restraints ($r_{\text{NH}\cdots\text{O}}$, 1.7–2.3; $r_{\text{N}\cdots\text{O}}$, 2.5–3.3) were used. Additionally, J-coupling constants (30), carbon chemical shifts of $\text{C}\alpha$ and $\text{C}\beta$ resonances (31), and a data base potential (32) (33) were directly included in the simulated annealing protocol during refinement.

Mutations and Measurements of Binding Affinity—At first, mutation sites were selected based on the structure of Fas death domain (19), but further mutations were made when an initial structure of FADD-DD was calculated. The mutation sites are in helices $\alpha 2$ and $\alpha 3$ and the connecting loop between them. Charged residues in $\alpha 2$ and $\alpha 3$ were replaced by Ala, and hydrophobic residues in the connecting loop were replaced by Asn similar to the *lpr* mutant of Fas. All mutants were single amino acid substitutions and purified as wild type FADD-DD described above. For the binding affinity measurements, human Fas-DD (Gly¹⁹²-Ser³⁰⁴) was expressed in *E. coli* and purified. The purified Fas-DD was coupled to sensor chip CM5 by amine coupling at pH 4.0 to get about 2,600 response units. In the same way, FADD was attached to a CM5 chip to have about 6,000 response units to measure self-association between FADD-DD and FADD. A flow of purified FADD-DD in HBS buffer (10 mM HEPES, pH 7.4, containing 150 mM NaCl, 3.4 mM EDTA, and 0.05% surfactant P20) at 5 different concen-

TABLE I
Summary of structural restraints derived from experimental measurements and structural statistics for the 20 final structures

NOE distance restraints	
Intra-residual	492
Sequential	291
Medium-range ($1 < i - j \leq 4$)	257
Long-range ($ i - j \geq 5$)	213
Hydrogen bonds	2*50 ^a
Angular restraints	
Dihedral angle ϕ	74
Dihedral angle ψ	66
Dihedral angle χ^1	34
Coupling constants	84
Chemical shifts	83
Ramachandran plot ^b (residues 6–93)	
Most favorable region	90.4 \pm 1.09
Additionally allowed region	7.2 \pm 1.29
Generously allowed region	2.4 \pm 0.62
Disallowed region	0.0 \pm 0.38
Atomic root mean square deviation values (\AA)	
Backbone atoms	0.35
Heavy atoms	0.89
X-PLOR energy terms (kcal/mol)	
E_{bond}	28.22 \pm 1.9
E_{angle}	210.33 \pm 6.18
E_{improper}	41.93 \pm 1.81
E_{vdw}	-741.75 \pm 42.97
E_{cdih}	0.47 \pm 0.18
E_{NOE}	215.37 \pm 11.52

^a For each hydrogen bond, two distance restraints are used, $r_{\text{HN}\cdots\text{O}}$ 1.7–2.3 and $r_{\text{N}\cdots\text{O}}$ 2.5–3.3. Coupling constants and chemical shifts are used for restraints based on Clore and co-workers (32). Chemical shifts restraints are ^{13}C chemical shifts of $\text{C}\alpha$ and $\text{C}\beta$ of each residue referenced from sodium 2,2-dimethyl-2-silapentane sulfonate at 30°C . Coupling constants are obtained from HNHA experiments.

^b The program PROCHECK_nmr (43) was used to analyze the quality of the structure. The values for X-PLOR energy terms were obtained with force constants of 4 kcal/mol/ \AA^4 (E_{vdw}), 50 kcal/mol/ \AA^2 (E_{NOE}), and 200 kcal/mol (E_{cdih}). E_{vdw} energy is L-J energy of X-PLOR energy terms.

trations between 55 to 880 nM was maintained over the protein-coupled chip for 2 min to record association at the flow rate of 20 $\mu\text{l}/\text{min}$. The bound FADD-DD was dissociated by passing HBS buffer without FADD-DD for the next 6 min at the same flow rate. Binding constants were obtained by BIAevaluation software (Biocore AB) using obtained sensorgrams. The degree of self-association was estimated based on the resonance signal obtained for 2 min of association. All binding experiments were performed at 25°C . All binding experiments were carried out with BIAcore 2000, and the N-terminal amino acid sequence of the purified protein was determined at Korea Basic Science Institute (KBSI) in Seoul.

RESULTS

Structure of FADD-DD—The structure of FADD-DD (residues 89–183) is well defined by 1,253 experimentally derived NOEs, 174 dihedral angle restraints, 50 hydrogen bonds, 84 coupling constants, and 83 additional chemical shifts (Table I). FADD-DD shown in Fig. 1 consists of 6 helices similar to other death domains of Fas (19) and the p75 neurotrophin receptor (34). Helices $\alpha 1$ and $\alpha 2$ are interlocked with helices $\alpha 4$ and $\alpha 5$, and helices $\alpha 3$ and $\alpha 6$ are located on each side. Helix $\alpha 6$ is well packed against the interlocked helices, but $\alpha 3$ is more loosely associated. Hydrophobic residues from $\alpha 1$, $\alpha 2$, $\alpha 4$, $\alpha 5$, and $\alpha 6$ form the hydrophobic core of the protein, but $\alpha 3$ is rather isolated from the others (Fig. 1). Most hydrophobic residues are well buried except for a few residues in $\alpha 1$ and $\alpha 6$. Helix $\alpha 2$ has mostly positively charged residues (Arg¹¹⁰, Lys¹¹³, Arg¹¹⁴, Arg¹¹⁷, and Lys¹²⁰) on the surface, whereas $\alpha 3$ has many negatively charged residues (Glu¹²³, Asp¹²⁷, Glu¹³⁰, and Glu¹³¹). Helices $\alpha 2$ and $\alpha 3$ form contiguous exposed charged surfaces with opposite polarity (Fig. 4). Helix $\alpha 4$ is relatively long compared with other helices, with a bend in the middle, and a 3¹⁰ helical turn is found between $\alpha 4$ and $\alpha 5$. Helices $\alpha 1$ and $\alpha 6$ have mostly negatively charged residues and a few hydrophobic residues on the surface (Fig. 1).

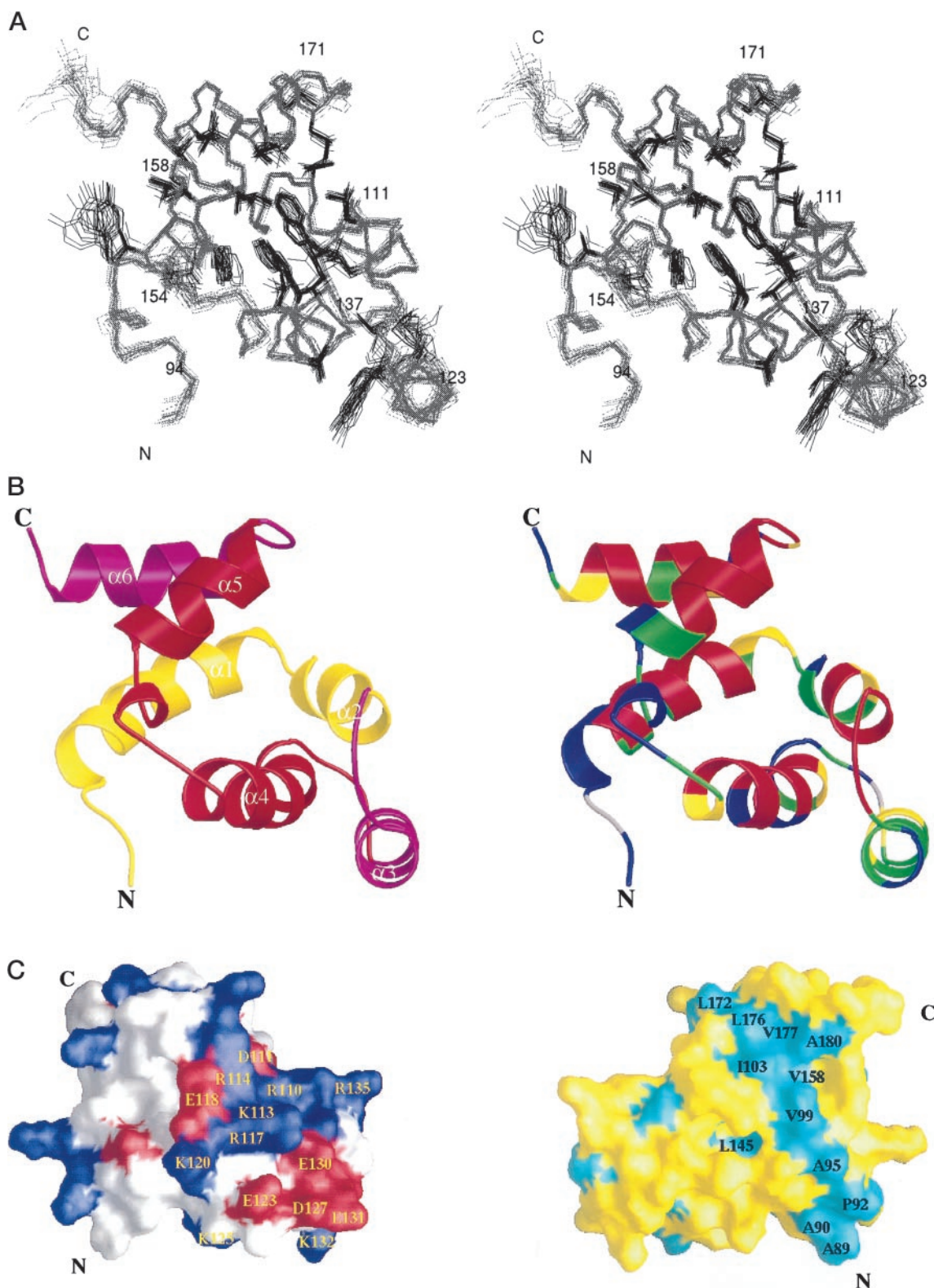


FIG. 1. **Structure of FADD-DD.** *A*, stereoview of the backbone atoms (N, Ca, C') of 20 structures of FADD-DD. The side chains of the hydrophobic residues are shown. The root mean square deviation about the mean coordinate position for residues 6–93 is 0.35 Å for the backbone atoms (N, Ca, C') and 0.89 Å for all heavy atoms. No distance restraints are violated more than 0.5 Å in any structures, and no torsion angle restraints are violated more than 5°. Other structural statistics are summarized in Table I. *B*, ribbon drawing of the averaged minimized NMR structure of FADD-DD. *C*, hydrogen exchange rates of FADD-DD backbone amide protons are color-coded. The slowest to fastest group is coded from red to blue. The slowest exchanging protons are distributed over helices $\alpha 1$ (Glu⁹⁴-Val¹⁰⁸), $\alpha 2$ (Asp¹¹¹-Glu¹¹⁸), $\alpha 4$ (Leu¹³⁷-Ala¹⁵¹), $\alpha 5$ (Val¹⁵⁸-Thr¹⁶⁷), and $\alpha 6$ (Leu¹⁷²-Gln¹⁸¹). Helix $\alpha 3$ (Glu¹²³-Lys¹³²) does not have any slowest exchanging protons. *D*, surface electrostatic potential is color-coded (left). The negative surface is in red ($< -8k_B T$), and the positive surface is in blue ($> 8k_B T$). The orientation is the same as in FADD-DD of Fig. 4. Surfaces with exposed hydrophobic residues such as Leu, Ile, Met, Val, Trp, Ala, and Phe is colored in sky blue (right). The orientation is rotated by 180° from the representation in the left. Ribbon drawing was generated by programs MOLSCRIPT (40) and RASTER3D (41), and electrostatic potential surface was generated by a program GRASP (42).

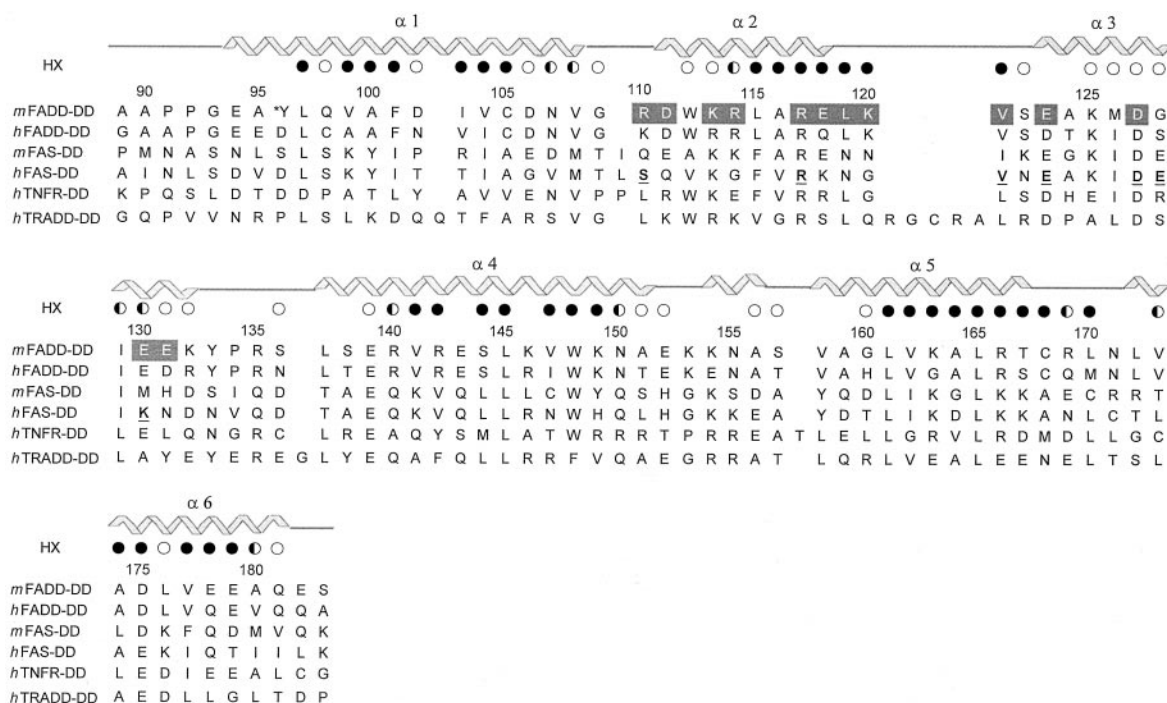


FIG. 2. Sequence alignments of death domains from mouse (m) FADD, human (h) FADD, mouse Fas, human Fas, human TNFR1, and human TRADD. Mutated residues in $\alpha 2$ and $\alpha 3$ are boxed. Hydrogen exchange rates are grouped into four classes. The slowest to the fastest exchanging protons are shown in filled circles, half-filled circles, open circles, and no symbols. The residues of Fas-DD involved in binding to FADD and self-association are underlined (19). *, mutation (Asp > Tyr) was found in a prepared sample.

Flexibility of FADD-DD—When hydrogen exchange rates of the backbone NHs were measured and classified into four classes by their exchange rates, each helix showed a different internal flexibility (Figs. 1 and 3). Helix $\alpha 3$ is the most flexible of all, and $\alpha 5$ is the least. Helix $\alpha 5$ in p75ICD (34) is also reported to be better protected from exchange compared with other helices, indicating that the organization of hydrophobic core of death domains is similar. Residues involved in the hydrophobic core formation are distributed over $\alpha 1$, $\alpha 2$, $\alpha 4$, $\alpha 5$, and $\alpha 6$, as are the slowly exchanging protons. The backbone NHs of the residues at the beginning of the helices, loop regions, and some exposed sides of the helices are exchanged in 30 min at 20 °C. The ϕ hydrogen bonds generally found at the end of the helices (35) are observed in FADD-DD, and the exchange rates of these hydrogen-bonded backbone NHs (Val¹²¹ and Leu¹⁷⁰) are protected; also, backbone NHs that have possible side chain N-cap interactions (Lys¹²⁵, Glu¹³⁹, Gly¹⁶⁰) were protected compared with the neighboring residues with unsatisfied NHs.

Binding Interactions between Fas-DD and FADD-DD—Because the global fold of FADD-DD is similar to that of Fas-DD and helices $\alpha 2$ and $\alpha 3$ of Fas-DD is known to be involved in FADD binding, we focused on $\alpha 2$ and $\alpha 3$. Mutants were constructed in which the charged residues in helices $\alpha 2$ and $\alpha 3$ were substituted by Ala, and Leu¹¹⁹ and Val¹²¹ were replaced by Asn (Fig. 2). The affinity of FADD-DD and variant proteins was measured by surface plasma resonance using BIAcore system (Pharmacia Biosensor AB). R110A, R113A, R117A, E118A, V121N, and E123A mutations virtually abolished the binding affinity of FADD-DD to Fas-DD, and R114A, L119N, and D127A mutations decreased the binding affinity more than four orders of magnitude (Fig. 3). All mutations decreased the binding affinity of FADD-DD but D111A, K120A, E130A, and E131A had marginal effects. All mutations constructed also decreased self-association of FADD. The association tendency can be divided into four classes based on self-association between FADD-DD and FADD. As indicated in Fig. 3, self-asso-

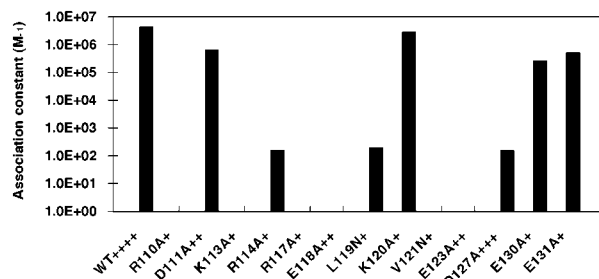


FIG. 3. Relative binding affinities of FADD-DD and its variants to Fas-DD. The binding affinity of each mutant is compared with wild type (WT) FADD-DD. Each mutant is constructed by replacing residues in helices $\alpha 2$ and $\alpha 3$ by either Ala or Asn. The binding affinities are shown in equilibrium association constants (K_a) at pH 7.4. The mutations shown with no binding constants (R110A, K113A, R117A, E118A, V121N, and E123A) reduced binding affinity of FADD-DD by more than 10,000-folds, and affinity could not be estimated because of the weak binding. Self-association was estimated based on the binding between FADD and FADD-DD after 2 min of association in 10 mM HEPES buffer containing 150 mM NaCl, 3.4 mM EDTA, and 0.05% surfactant P20 at 25 °C. +, the self-association tendencies are indicated from the highest (++++) to the lowest (+).

ciation is also significantly alleviated by the mutations in helices $\alpha 2$ and $\alpha 3$, indicating that self-association and binding to Fas-DD use similar surface. These results indicate that the charged residues in $\alpha 2$ and $\alpha 3$ are involved in Fas interaction and self-association, which is also shown in Fas-DD (19).

DISCUSSION

The structure of FADD-DD (Fig. 1) indicates that its fold is similar to other death-related proteins such as Fas-DD (19), FADD-DED (20), and caspase recruitment domain of RAIDD (21). Helices $\alpha 1$, $\alpha 2$, $\alpha 4$, $\alpha 5$, and $\alpha 6$ form a hydrophobic core, and helix $\alpha 3$ is somewhat isolated from the rest of the protein and is the most flexible among the helices. Considering that $\alpha 2$ and $\alpha 3$ are involved in the binding to Fas-DD, $\alpha 3$ is most likely to be involved in binding modulation and adapter protein se-

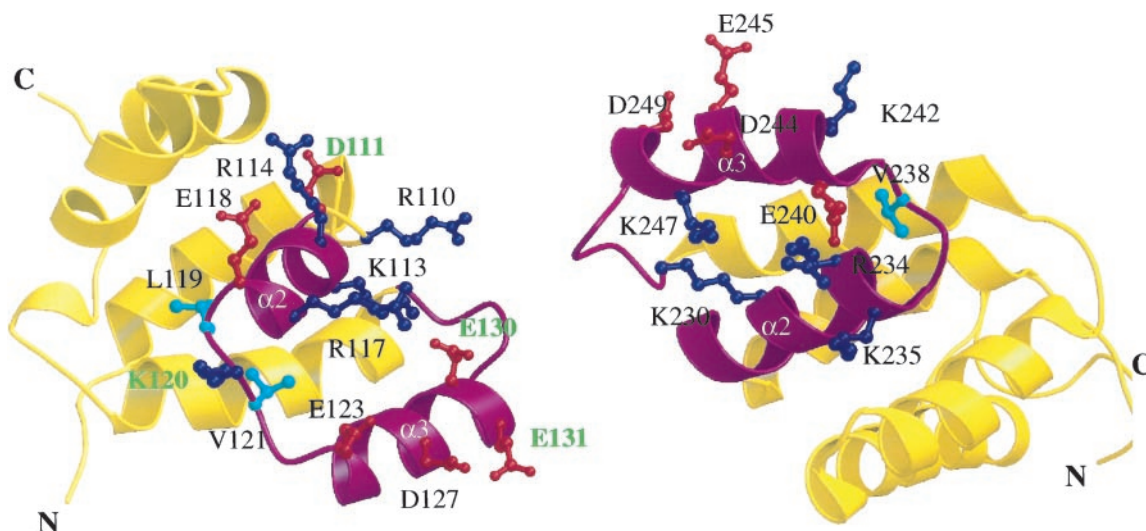


FIG. 4. The structure of proposed interaction sites of FADD-DD (left) and Fas-DD (19) (right). Positively charged residues are colored in blue, negatively charged residues are colored in red, and two hydrophobic residues (Leu¹¹⁹, Val¹²¹) are colored in sky blue. Only residues of FADD-DD studied by mutations are labeled. Residues with marginal effect on binding to Fas-DD are labeled in green. Val¹²¹ is the corresponding residue at the position of *lpr* mutant in Fas. Helices $\alpha 2$ and $\alpha 3$ in FADD-DD and Fas-DD have the same charge distribution, suggesting that interaction between two death domains is in antiparallel pattern.

lectivity. The flexibility of $\alpha 3$ could be crucial in maximizing contacts between the interacting death domains. The *lpr* mutation in Fas receptor induces the complete loss of $\alpha 3$ and reduces the binding affinity of Fas-DD to FADD (36), and the corresponding mutation (V121N) in FADD-DD also showed similar loss in binding affinity. This may indicate that the role of $\alpha 3$ is conserved in death domains. FADD-DD structure has an exposed hydrophobic surface at the N- and C-terminal helices (Fig. 1), and the same pattern was reported in FADD-DED (20). Because the C terminus of DED is connected to the N terminus of DD in an intact FADD, the structure of FADD would have 12 antiparallel helices comprising 6 helices from each domain and a disordered C terminus comprising residues 184–205. The interactions between DED and DD domains are expected to be from the residues of $\alpha 1$ and $\alpha 6$ of each domain. The partial digestion of FADD by subtilisin indicates that the C-terminal region comprising residues 184–205 is the most susceptible to the protease. Also the fragments that remained intact after 2 h of digestion were the N-terminal 88 residues (residues 1–88) and the C-terminal 95 residues (residues 89–183), indicating that two domains are connected by a flexible loop.

Mutations of charged residues in $\alpha 2$ and $\alpha 3$ of FADD-DD indicate that the major binding sites between FADD-DD and Fas-DD appear to reside in $\alpha 2$ and $\alpha 3$. Mutations of Fas-DD (19), TNFR-DD (37), and TRADD-DD (38) indicated that $\alpha 2$ and $\alpha 3$ are important for functions, but other regions are also implicated. However, among the residues on the surface, charged residues in $\alpha 2$ and $\alpha 3$ are most likely candidates for protein interactions. Other residues affecting the structural integrity of death domains, such as *lpr* mutant, could have effects on protein functions. The result of extensive mutation studies in $\alpha 2$ and $\alpha 3$ of FADD-DD indicates that this region affects binding affinity of Fas-DD for FADD-DD. As shown in Fig. 4, the charge distribution in $\alpha 2$ and $\alpha 3$ of FADD-DD and Fas-DD are similar, indicating that interactions between the two proteins are anti-parallel. Helix $\alpha 2$ of Fas-DD interacts with $\alpha 3$ of FADD-DD and *vice versa*.

In Fas-induced apoptosis, Fas receptor is trimerized upon stimulation and then recruits FADD. It is not known yet whether Fas receptor trimer is needed for creating a binding site for FADD, or trimerization is a means to expose the extra

binding surface of Fas receptor to FADD. Our experiments showed that FADD-DD binds to Fas-DD with a dissociation constant of about 200 nM. Considering that FADD and Fas used in experiments are mouse and human origin, respectively, and the fact that Fas-DD binds better to an intact FADD (39) than FADD-DD alone, Fas receptor monomer seems to be capable of recruiting FADD. This indicates that the trimerization of Fas receptor is required to expose a binding surface rather than creating a binding surface. The whole binding surface of Fas-DD may not be available in monomer either by interacting with membrane or other factors. When induced by ligand, the whole binding surface of Fas-DD would be exposed by conformational change and recruit FADD. Once the death domain of Fas binds to FADD, the induced conformational change (3) would convert FADD into a high affinity form for procaspase-8, triggering recruitment and activation of caspase-8. The mode of conformational change is not clear, but domain movement of DD and DED of FADD is most likely. However, the low affinity binding between DDs or DEDs may occur in a normal cell, so overexpression of proteins containing these domains can lead to cell death. In fact, the difference in affinity between the low affinity and the high affinity form of Fas receptor or FADD may not be that high. The 10-fold difference in binding affinity is equivalent to about 1.3 kcal/mol at the physiological temperature, indicating that a small conformational change can easily switch from the low affinity to high affinity form.

In conclusion, FADD death domain consists of six antiparallel helices similar to other known death-related domains. Helices $\alpha 2$ and $\alpha 3$ of death domain constitute a major binding surface and appear to interact antiparallel with the death domain of Fas receptor. We think that the ligand-induced exposure of the binding site of Fas receptor and FADD is crucial to Fas-mediated apoptosis.

Acknowledgment—We thank Professor B. Sykes for letting us use the NMR in his laboratory, Drs. S. Gagné and K. B. Lee for the help with NMR experiments, Drs. K. Rajarathnam and C. Woodward for critical reading and comments, Dr. D. Garrett for the PIPP program, Dr. L. Kay for pulse sequences, and Dr. G. M. Clore for the data base potential library.

REFERENCES

- Chinnaiyan, A. M., O'Rourke, K., Tewari, M., and Dixit, V. M. (1995) *Cell* **81**, 505–512

2. Zhang, J., and Winoto, A. (1996) *Mol. Cell. Biol.* **16**, 2756–2763
3. Muzio, M., Chinnaiyan, A. M., Kischkel, F. C., O'Rourke, K., Shevchenko, A., Ni, J., Scaffidi, C., Bretz, J. D., Zhang, M., Gentz, R., Mann, M., Krammer, P. H., Peter, M. E., and Dixit, V. M. (1996) *Cell* **85**, 817–827
4. Yang, X., Chang, H. Y., and Baltimore, D. (1998) *Mol. Cell* **1**, 319–325
5. Muzio, M., Stockwell, B. R., Stennicke, H. R., Salvesen, G. S., and Dixit, V. M. (1998) *J. Biol. Chem.* **273**, 2926–2930
6. Kischkel, F. C., Hellbardt, S., Behrmann, I., Germer, M., Pawlita, M., Krammer, P. H., and Peter, M. E. (1995) *EMBO J.* **14**, 5579–5588
7. Medema, J. P., Scaffidi, C., Kischkel, F. C., Shevchenko, A., Mann, M., Krammer, P. H., and Peter, M. E. (1997) *EMBO J.* **16**, 2794–2804
8. Hsu, H., Shu, H. B., Pan, M. G., and Goeddel, D. V. (1996) *Cell* **84**, 299–308
9. Thome, M., Schneider, P., Hofmann, K., Fickenscher, H., Meink, E., Neipel, F., Mattmann, C., Burns, K., Bodmer, J. L., Schroter, M., Scaffidi, C., Krammer, P. H., Peter, M. E., and Tschopp, J. (1997) *Nature* **386**, 517–521
10. Hu, S., Vincenz, C., Buller, M., and Dixit, V. M. (1997) *J. Biol. Chem.* **272**, 9621–9624
11. Bertin, J., Armstrong, R. C., Otilie, S., Martin, D. A., Wang, Y., Banks, S., Wang, G. H., Senkevich, T. G., Alnemri, E. S., Moss, B., Lenardo, M. J., Tomaselli, K. J., and Cohen, J. I. (1997) *Proc. Natl. Acad. Sci. U. S. A.* **94**, 1172–1176
12. Irmeler, M., Thome, M., Hahne, M., Schneider, P., Hofmann, K., Steiner, V., Bodmer, J. L., Schroter, M., Burns, K., Mattmann, C., Rimoldi, D., French, L. E., and Tschopp, J. (1997) *Nature* **388**, 190–195
13. Goltsev, Y. V., Kovalenko, A. V., Arnold, E., Varfolomeev, E. E., Brodianskii, V. M., and Wallach, D. (1997) *J. Biol. Chem.* **272**, 19641–19644
14. Scaffidi, C., Schmitz, I., Krammer, P. H., and Peter, M. E. (1999) *J. Biol. Chem.* **274**, 1541–1548
15. Yeh, W. C., Pompa, J. L., McCurrach, M. E., Shu, H. B., Elia, A. J., Shahinian, A., Ng, M., Wakeham, A., Khoo, W., Mitchell, K., El-Deiry, W. S., Lowe, S. W., Goeddel, D. V., and Mak, T. W. (1998) *Science* **279**, 1954–1958
16. Zhang, J., Cado, D., Chen, A., Kabra, N. H., and Winoto, A. (1998) *Nature* **392**, 296–300
17. Wiegmann, K., Schwandner, R., Krut, O., Yeh, W.-C., Mak, T. W., and Kronke, M. (1999) *J. Biol. Chem.* **274**, 5267–5270
18. Chinnaiyan, A. M., Tepper, C. G., Seldin, M. F., O'Rourke, K., Kischkel, F. C., Hellbardt, S., Krammer, P. H., Peter, M. E., and Dixit, V. M. (1996) *J. Biol. Chem.* **271**, 4961–4965
19. Huang, B., Eberstadt, M., Olejniczak, E. T., Meadows, R. P., and Fesik, S. W. (1996) *Nature* **384**, 638–641
20. Eberstadt, M., Huang, B., Chen, Z., Meadows, R. P., Ng, S. C., Zheng, L., Lenardo, M. J., and Fesik, S. W. (1998) *Nature* **392**, 941–945
21. Chou, J. J., Matsuo, H., Duan, H., and Wagner, G. (1998) *Cell* **94**, 171–180
22. Zhang, O., Kay, L. E., Olivier, J. P., and Forman-Kay, J. D. (1994) *J. Biomol. NMR* **4**, 845–858
23. Kuboniwa, H., Grzesiek, S., Delaglio, F., and Bax, A. (1994) *J. Biomol. NMR* **4**, 871–878
24. Pascal, S. M., Muhandiram, D. R., Yamazaki, T., Forman-Kay, J. D., and Kay, L. E. (1994) *J. Magn. Reson. Ser. B* **103**, 197–201
25. Muhandiram, D. R., and Kay, L. E. (1994) *J. Magn. Reson. Ser. B* **103**, 203–216
26. Kay, L. E., Xu, G.-Y., Singer, A. U., Muhandiram, D. R., and Forman-Kay, J. D. (1993) *J. Magn. Reson. B* **101**, 333–337
27. Delaglio, F., Grzesiek, S., Vuister, G. W., Zhu, G., Pfeifer, J., and Bax, A. (1995) *J. Biomol. NMR* **6**, 277–293
28. Clore, G. M., Bax, A., and Gronenborn, A. M. (1991) *J. Biomol. NMR* **1**, 13–22
29. Wüthrich, K., Billeter, M., and Braun, W. (1983) *J. Mol. Biol.* **169**, 949–961
30. Garrett, D. S., Kuszewski, J., Hancock, T. J., Lodi, P. J., Vuister, G. W., Gronenborn, A. M., and Clore, G. M. (1994) *J. Magn. Reson. Ser. B* **104**, 99–103
31. Kuszewski, J., Qin, J., Gronenborn, A. M., and Clore, G. M. (1995) *J. Magn. Reson. Ser. B* **106**, 92–96
32. Kuszewski, J., Gronenborn, A. M., and Clore, G. M. (1996) *Protein Sci.* **5**, 1067–1080
33. Kuszewski, J., Gronenborn, A. M., and Clore, G. M. (1997) *J. Magn. Reson.* **125**, 171–177
34. Liepinsh, E., Ilag, L. L., Otting, G., and Ibanez, C. F. (1997) *EMBO J.* **16**, 4999–5005
35. Kabsch, W., and Sander, C. (1983) *Biopolymers* **22**, 2577–2637
36. Eberstadt, M., Huang, B., Olejniczak, E. T., and Fesik, S. W. (1997) *Nat. Struct. Biol.* **4**, 983–985
37. Tartaglia, L. A., Ayres, T. M., Wong, G. H., and Goeddel, D. V. (1993) *Cell* **74**, 845–853
38. Park, A., and Baichwal, V. R. (1996) *J. Biol. Chem.* **271**, 9858–9862
39. Boldin, M. P., Goncharov, T. M., Goltsev, Y. V., and Wallach, D. (1996) *Cell* **85**, 803–815
40. Kraulis, P. J. (1991) *J. Appl. Crystallogr.* **24**, 946–950
41. Merritt, E. A., Bacon, D. J., and David, J. (1997) *Methods Enzymol.* **277**, 505–524
42. Nicholls, A., Sharp, K. A., and Honig, B. (1991) *Proteins* **11**, 281–296
43. Laskowski, R. A., Rullmann, J. A., MacArthur, M. W., Kaptein, R., and Thornton, J. M. (1996) *J. Biomol. NMR* **8**, 477–486